Asian J. Energy Environ., Vol. 5, Issue 3, (2004), pp. 171-196

PV Water Pumping System Using a Current-Fed Parallel Resonant Push-Pull Inverter for Rural Area Applications

D. C. Martins*, M. Mezaroba, O. H. Gonçalves and A. S. de Andrade

Federal University of Santa Catarina
Power Electronics Institute - INEP
P.O. BOX 5119 - 88.040-970 - Florianópolis - SC - Brazil
*Corresponding author: Tel.: 55(48)231-9204; Fax: 55(48)234-5422
E-mail: denizar@inep.ufsc.br

(Received : 31 January 2004 – Accepted : 15 March 2004)

Abstract: This paper presents the analysis of a water pumping system from photovoltaic cells using a current-fed parallel resonant push-pull inverter, for residential applications in rural areas. The structure of the power circuit is particularly simple and robust. It works in a ZVS commutation. Its main features are: one power processing stage, simple control strategy, low harmonic distortion of the load voltage, and natural isolation. The principle of operation, design procedure and experimental results are presented.

Keywords: PV Water Pumping System, Resonant Converter, Push-Pull Inverter, PWM Modulation, PV Solar Cells.

Introduction

The increasing research to discover alternative means for obtaining electrical energy in a simple manner, without pollution, that at the same time do not cause a hard ecological impact on the environment, has led some professionals of the electrical engineering area to opt for solar energy conversion.

This kind of energy, apparently unfailing, presents a series of advantages, among them we can point out: non-aggression to natural conditions, and no cause of any type of pollution. However, its treatment for industrial applications and even for residential ones still represents a relatively high cost. Nowadays studies in the conception and materials manufacture area for photovoltaic cells are rapidly being developed with great success. The main objective is to obtain systems for converting solar energy into electrical energy in a simple, cheap and safe way.

Considering the objective mentioned above, this paper describes a system for residential applications in rural areas, where power from a utility is not available or is too costly to install. The system consists of water pumping from photovoltaic cells using a current-fed parallel resonant push-pull inverter with battery storage.

Much work in the PV water pumping area for residential applications, is available in technical literature. The majority of them use an AC or DC machine to drive the water pump [1,2,3,4]. The main inconvenience presented by these systems are: low efficiency, high reactive power circulation, expensive maintenance, complex electronic drive circuits, large volume, and high weight and cost. These items are particularly serious in rural applications, in which maintenance, simplicity and cost must be optimized.

The system proposed in this work uses a vibratory under-water pump that consists of an electromagnet circuit, which produces a vibration in a diaphragm with the same operation frequency of the electromagnet circuit.

The studies realized during this work show that the current-fed parallel resonant push-pull inverter is very well adapted to this kind of load (vibratory under-water pump) [8]. It naturally generates a high quality sinusoidal voltage waveform across the pump, with ZVS commutation. This strategy permits simple and safe operation of the whole system.

The main advantages of the proposal mentioned above are: absence of any rotating mechanical part, that diminishes the wear and tear of pump pieces and augments the efficiency of the system, robustness, low maintenance, simplicity of the control drive circuit, easy installation and operation, low weight, volume and cost.

Equivalent Electric Model of the Vibratory Under-Water Pump

For rural area application the vibratory under-water pump is particularly recommended due its simplicity, low cost and robustness. Besides, this pump can effect the pumping in well with profundity around 80 metres. Under normal conditions the pumping is approximately 1500 litres per hour. In Figure 1 we can observe the behavior of the pump for various profundities.

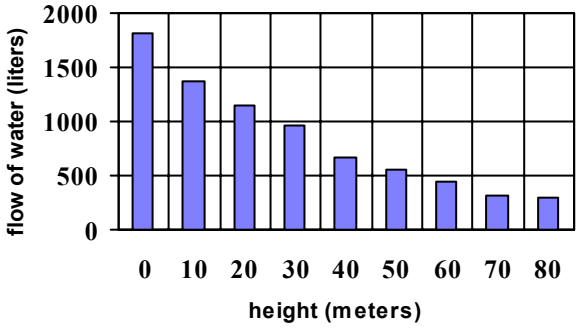

Figure 1. Performance of the water pump.

The technical characteristics of the pump are shown in Table 1. The equivalent electric model is obtained experimentally, connecting the pump directly to the utility. Figures 2 and 3 show the waveforms of the voltage and current in the pump. The equivalent electric model is presented in Figure 4, obtained from the dates given below and the equations (1) and (2).

- $Vin = 217.8V$ (Utility rms voltage);
- $Ip = 4.9A$ (Pump rms current);

- $\phi = 74.68^{o}$ (Phase angle);
- $f = 60Hz$ (Operation frequency of the pump).

Table 1. Technical characteristics of the water pump.

Model	BK N^{o} 3 - 80m
System	Vibratory
Apparent Power	1,100 VA
RMS Voltage	220 V
Frequency	60 Hz
Pressure Tube	3/4”
Weight	5.5 Kg
Flow of Water	1800 litres

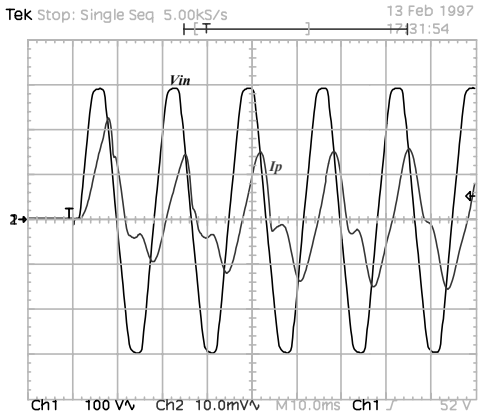

Figure 2. Voltage and current in the pump (Start condition). Scale: 100V/div; 5A/div; 10ms/div.

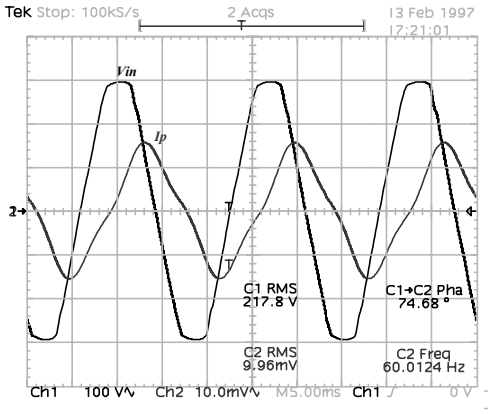

Figure 3. Voltage and current in the pump (Steady-state condition). Scale: 100V/div; 5A/div; 5ms/div.

We can verify that the load (pump) has an inductive characteristic, with large circulation of reactive energy and low power factor (*cos* ϕ). Therefore, an equivalent parallel RL circuit (Fig.4) can easily represent the electric model of the pump, where:

$$R_p = \frac{V_{in}}{I_p \cdot \cos\phi} = 170\Omega \qquad (1)$$

$$L_p = \frac{V_{in}}{2 \cdot \pi \cdot f \cdot I_p \cdot \sin\phi} = 120mH \qquad (2)$$

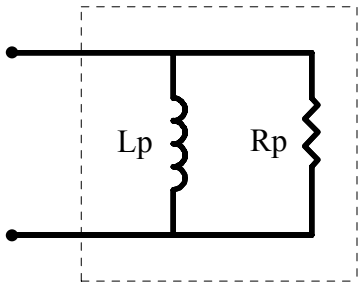

Figure 4. Electric model of the pump.

Principle of Operation

Considering the application mentioned in this paper the Current-Fed Self-Oscillator Parallel Resonant Push-Pull Inverter is proposed, in which the resonant capacitor is connected in parallel with the load (pump), in the secondary side of the transformer. This strategy is very convenient, because the reactive energy stays confined in the resonant output circuit, permitting that the push-pull inverter circuit processes only the active power demanded by the pump. This circuit is based on the topologies presented in [5, 6, 7]. Mosfets were used for the main switches, simplifying the self-oscillator drive circuit. The complete structure, including the self-oscillator drive circuit, is shown in Figure 5. To simplify the analysis, the following assumptions are made: the operation of the circuit is steady-state; the semiconductors are considered ideal; the transformer is represented by its magnetizing inductance; and the input current is maintained constant without ripple. The parallel resonant push-pull inverter has two operation stages shown in Figures 6 and 7.

1. Operation Stages

1st Stage (t_0, t_1) - Fig. 6: This stage starts in t_0. When the voltage *Vout* reaches zero the switch S_1 turns off and the switch S_2 turns on instantaneously. The commutation of the switches occurs at zero voltage. Due to the resonance between C_r and L_p, *Vout* increases sinusoidally.

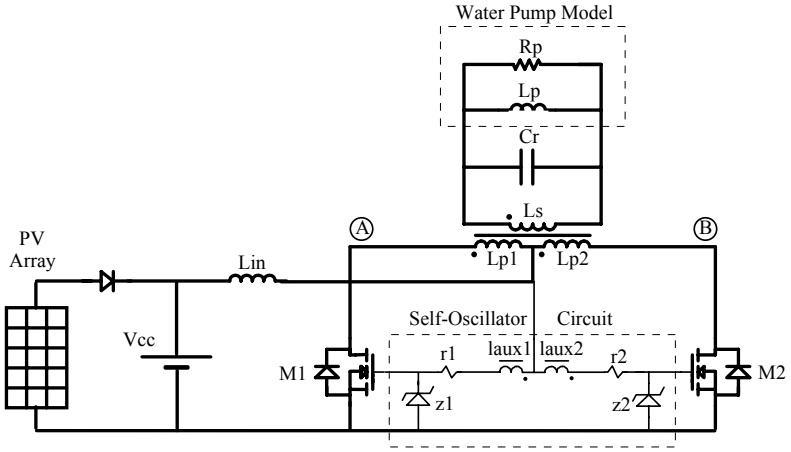

Figure 5. Proposed Structure.

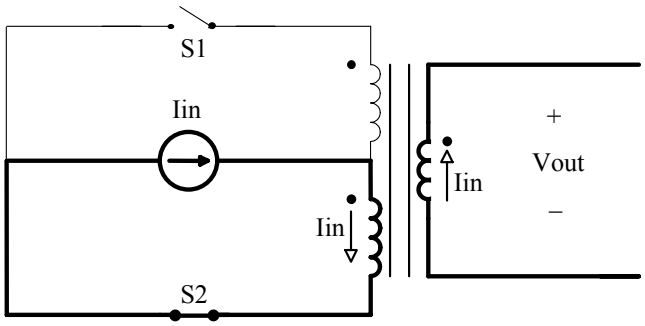

Figure 6. 1st stage.

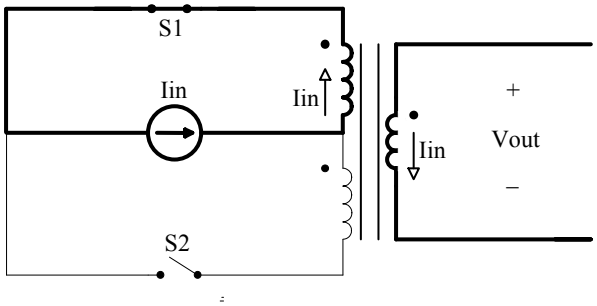

Figure 7. 2nd stage.

2nd Stage (t_1, t_2) - Figure 7: At the time t_1, the switch S_2 turns off and the switch S_1 turns on. The voltage *Vout* decreases sinusoidally until the time t_2, where a new operation period restarts. The main waveforms are shown in Fig.8.

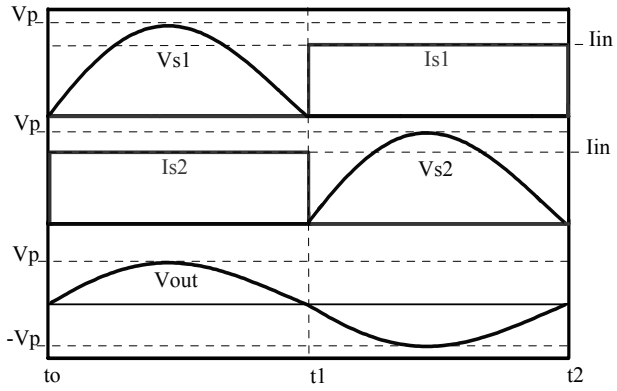

Figure 8. Main waveforms.

Mathematical Analysis

Before formulating a design methodology for the proposed converter, it is necessary to develop the main circuit equations. To simplify the mathematical analysis the following assumptions are made: the inductor *Lin* is much bigger than the inductors *Lp1*, *Lp2*; the transformer and all components are considered ideals.

The voltage across the primary winding of the transformer is proportional to the input voltage. Due to the modulation of the drive circuitry with a signal from the resonant tank (Fig. 5) a sinusoidal voltage waveform of high quality is generated from

point A to B. The relationship between the *rms* voltage V_{AB} and the DC input voltage *Vcc* is given by:

$$V_{AB(rms)} = \frac{V_{cc} \cdot \pi}{\sqrt{2}} \tag{3}$$

The transformer turns ratio *a* results in:

$$a = \frac{Vout_{(rms)}}{V_{AB(rms)}} \tag{4}$$

where $Vout_{(rms)}$ is the *rms* output voltage. Then, all the output impedances are referred to the primary side of the transformer as:

$$C = C_r \cdot a^2 \rightarrow \text{ reflected resonant capacitor} \tag{5}$$

$$L = \frac{L_p}{a^2} \rightarrow \text{ reflected output inductor} \tag{6}$$

$$R = \frac{R_p}{a^2} \rightarrow \text{ reflected output resistor} \tag{7}$$

If the transformer has a low magnetizing inductance (L_m), it is convenient to take the equivalent inductance (L_{eq}) as a parallel between the magnetizing inductance and the load inductance (L_p). However, most cases $L_m >> L_p$, and $L_{eq} \approx L_p$. The simplified equivalent circuit can be observed in Figure 9.

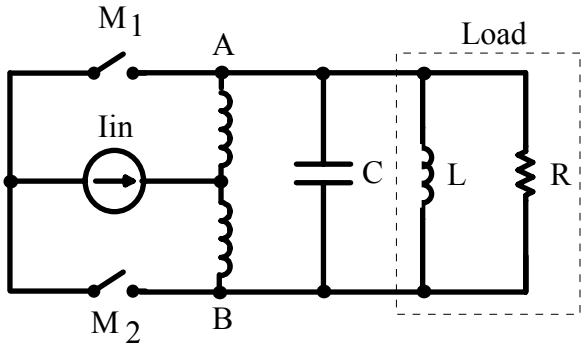

Figure 9. Simplified equivalent circuit.

So, the average input current of the converter can be expressed by:

$$I_{in} = \frac{V_{cc} \cdot a^2 \cdot \pi^2}{2 \cdot R_p \cdot \eta} \qquad (8)$$

where η represents the efficiency of the converter.

The peak voltage across the switches can be determined by:

$$V_{S(peak)} = V_{AB(peak)} = V_{CC} \cdot \pi \qquad (9)$$

From Fig. 8 the *rms* current through the switches can be obtained. So:

$$I_{S(rms)} = \frac{I_{in}}{\sqrt{2}} \qquad (10)$$

If we consider the alternating switching operation, the circuit of Figure 9 can be equivalently redrawn as shown in Fig. 10 [5], where the waveform of the input current of the converter is symmetrical and the duty cycle is equal to 0.5. The differential equation that represents the new equivalent circuit is given below:

$$C \cdot \frac{d^2 v_{AB}}{dt^2} + \frac{1}{R} \cdot \frac{dv_{AB}}{dt} + \frac{1}{L} = 0 \tag{11}$$

where $v_{AB}(t) = v_C(t) \rightarrow$ capacitor voltage (12)

The resonance frequency is given by the following equation:

$$\omega_o = \frac{1}{\sqrt{L \cdot C}} \tag{13}$$

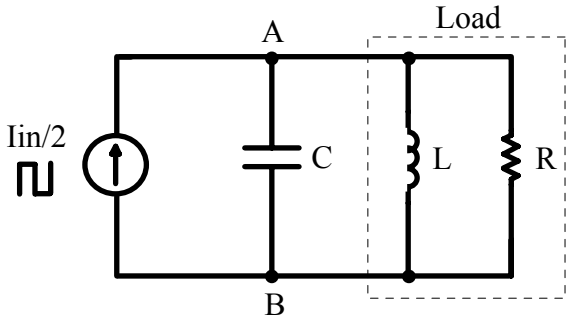

Figure 10. New equivalent circuit.

The converter works in a ZVS condition, that is, when the voltage across the capacitor *C* reaches zero the commutation occurs. So, the initial conditions of the circuit are: $v_C(0) = 0$; $i_L(0) = I_{L_o}$.

Substituting the initial conditions in equation (11), we can obtain the following results:

$$v_{C(t)} \frac{I_{in}/2 - I_{L_o}}{C \cdot \omega} \cdot e^{-\alpha \cdot t} \cdot \sin(\omega t) \tag{14}$$

$$i_{L(t)} \frac{I_{in}/2 - I_{L_o}}{L \cdot C \cdot \omega} \left[\frac{-\omega}{{\omega_o}^2} \cdot e^{-\alpha \cdot t} \cdot \cos(\omega t) - \frac{-\alpha}{{\omega_o}^2} \cdot e^{-\alpha \cdot t} \cdot \sin(\omega t) \right] \tag{15}$$

$$\text{where: } \omega^2 = {\omega_o}^2 - \alpha^2 \; ; \; \alpha = \frac{1}{2 \cdot R \cdot C} ; \; \alpha^2 << {\omega_o}^2 \tag{16}$$

For each half-cycle ($\omega/2$) the capacitor voltage crosses zero. In that moment the commutation of the switches take place.

The capacitance of the resonant capacitor is obtained associating the equations (13) and (16). Thus:

$$C = \frac{4 \cdot R^2 + \sqrt{16 \cdot R^4 - 16 \cdot R^2 \cdot L^2 \cdot \omega^2}}{8 \cdot R^2 \cdot L \cdot \omega^2} \tag{17}$$

Design Procedures and Example

1. Specifications

Input Data:

Vcc = 12V (Converter input voltage)

Water Pump Data:

Vout = 220 (rms voltage)

Sout = 1085 VA (apparent power)

Pout = 281 W (active power)

Lp = 120 mH (equivalent parallel inductance)

Rp = 170 Ω (equivalent parallel resistance)

f = 60 Hz (operation frequency) $\Rightarrow$ ω = 377 rad/s

η = 80% (efficiency)

2. RMS V_{AB} voltage

The *rms* V_{AB} voltage is given by the following equation:

$$V_{AB(rms)} = \frac{Vcc \cdot \pi}{\sqrt{2}} = 26.65\ V \tag{18}$$

3. Transformer Turns Ratio (a).

$$a = \frac{Vout_{(rms)}}{V_{AB(rms)}} = 8.25 \tag{19}$$

4. Magnetizing inductance referred to the secondary side of the transformer (Lm_{sec})

$$\mathrm{Im}_{\mathrm{sec}} = 0.1 \cdot \frac{Sout}{Vout} \tag{20}$$

$$Lm_{\mathrm{sec}} = \frac{a \cdot V_{ABrms}}{\omega \cdot \mathrm{Im}_{\mathrm{sec}}} = 1.19\ H \tag{21}$$

where: $Im_{sec} \rightarrow$ magnetizing current referred to the secondary side of the transformer.

5. Input current and inductor (I_{in}, L_{in})

$$Iin = \frac{V_{AB(rms)}.a^2 \cdot \pi}{R_p \cdot \sqrt{2} \cdot \eta} = 29.6\ A \tag{22}$$

$$Lin = \frac{Vcc \cdot T/4}{0.1 \cdot Iin} = 17\ mH \tag{23}$$

where: $T = 1/f$

6. Resonant Capacitor (Cr)

$$Cr = \frac{4.Rp^2 + \sqrt{16.Rp^4 - 16.Rp^2.Leq^2.\omega^2}}{8.Rp^2.Leq.\omega^2} = 63.6\ \mu F \tag{24}$$

where: $Leq = Lp//Lm_{sec}$

7. Number of Parallel Batteries

The average power and current delivered by the batteries will be:

$$P_{Bav} = \frac{Pout}{\eta} \cong 350W \tag{25}$$

$$I_{Bav} = \frac{P_{Bav}}{Vcc} \cong 30A \tag{26}$$

The number of parallel batteries is given by:

$$N_B = \frac{B_A \cdot I_{Bav}}{B_c} = 1.5 \text{ batteries} \tag{27}$$

where:

$N_B \rightarrow$ minimum number of parallel batteries,

$B_A \rightarrow$ battery autonomy: 3 hours,

$B_C \rightarrow$ battery capacity: 60Ah (one-hour rate).

Two lead-acid batteries (12V - 100Ah (20 hours rate)) were chosen.

8. Number of Photovoltaic Modules

The photovoltaic modules used in the design can deliver 3Ah (Ampere-hours) with a solar radiation of 1.000 W/m^2. In the worst case the average solar radiation, in our region (Florianópolis/Santa Catarina – Brazil), is about 2500 W/m^2 per day. Thus:

$$Ah_d = \frac{I_{Rs} \cdot R_{av}}{R_s} = 7.5\ Ah \qquad (28)$$

where:

$Ah_d \rightarrow$ Ampere-hours delivery per photovoltaic module for one day.

$R_{av} \rightarrow$ average solar radiation: 2500 W/m^2 / day (worst situation),

$R_S \rightarrow$ standard solar radiation: 1000 W/m^2,

$I_{RS} \rightarrow$ delivery of current by the photovoltaic module for the R_{av} radiation: 3Ah.

Thus, the number of photovoltaic modules is given by:

$$Np = \frac{Ah_L}{Ah_d} = 4\ photovoltaic\ modules \qquad (29)$$

where: $Ah_L \rightarrow$ Ampere-hours delivery to the load per day.

Simulation Results

In order to evaluate the employed methodology, some numerical simulations of the system were made using the PSPICE program [9], following the same specifications and the same design outlined in the preceding section.

The main results are shown in the following figures:

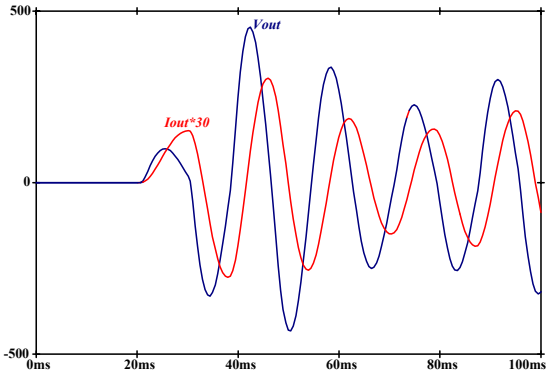

Figure 11. Voltage and current in the pump (Start-transient).

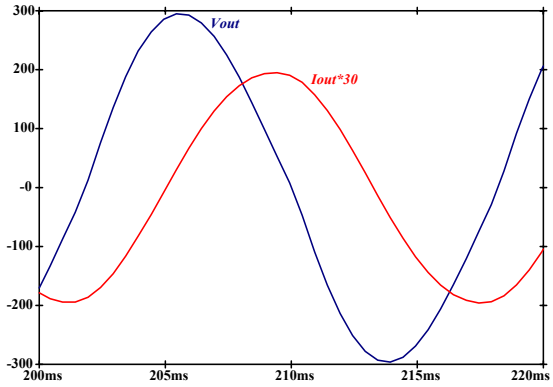

Figure 12. Voltage and current in the pump (Steady-state condition).

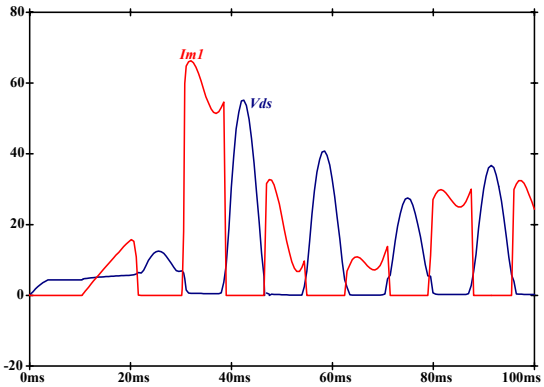

Figure 13. Voltage and current in the main switches (Start-transient).

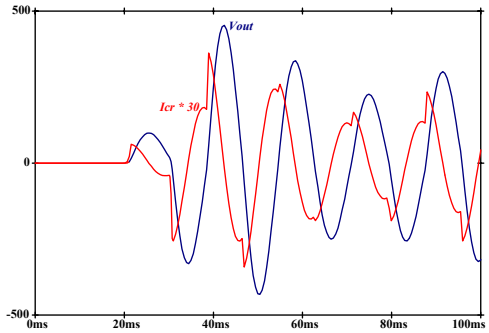

Figure 14. Voltage and current in the resonant capacitor (Start transient).

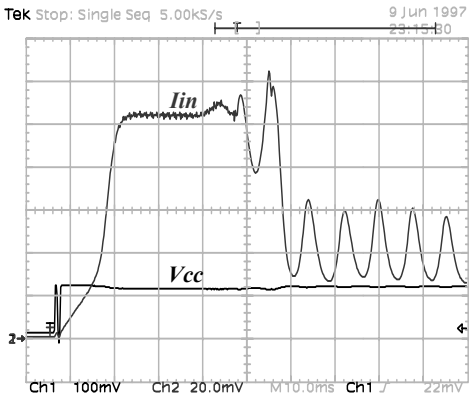

Figure 15. Voltage and current in the batteries (Start-transient)
Scales: 10V/div; 20A/div; 10ms/div.

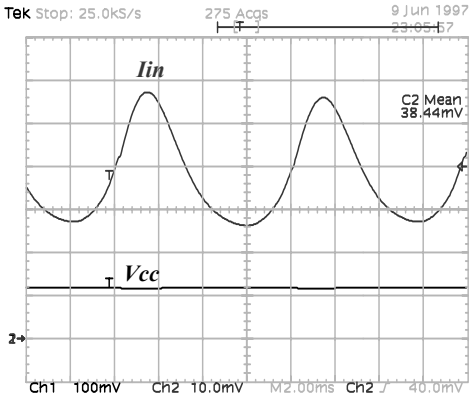

Figure16. Voltage and current in the batteries (Steady-state condition)
Scale: 10V/div; 10A/div; 2ms/div.

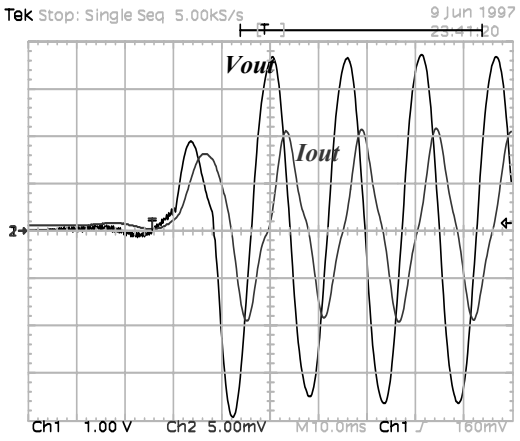

Figure 17. Voltage and current in the pump
(Start-transient)
Scale: 100V/div; 5A/div; 10ms/div.

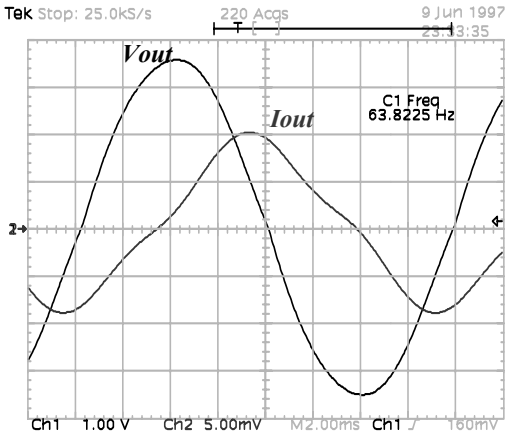

Figure 18. Voltage and current in the pump
(Steady-state condition)
Scale: 100V/div; 5A/div; 2ms/div.

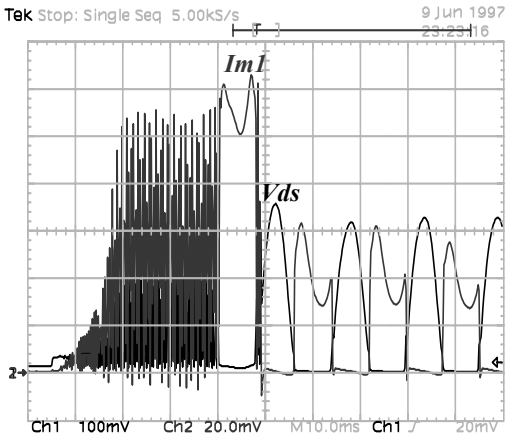

Figure 19. Voltage and current in the main switches (Start-tranient).
Scale: 10V/div; 20A/div; 10ms/div.

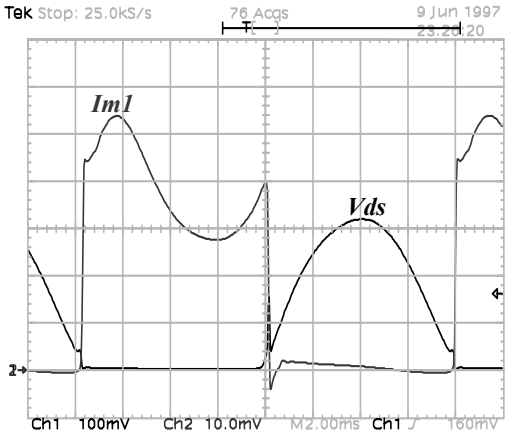

Figure 20. Voltage and current in the main switches (Steady-state condition)
Scale: 10V/div; 10A/div; 2ms/div.

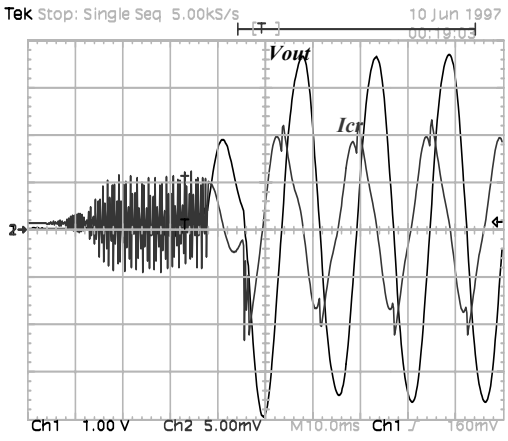

Figure 21. Voltage and current in the resonant capacitor (Start-transient).
Scale: 100V/div; 5A/div; 10ms/div.

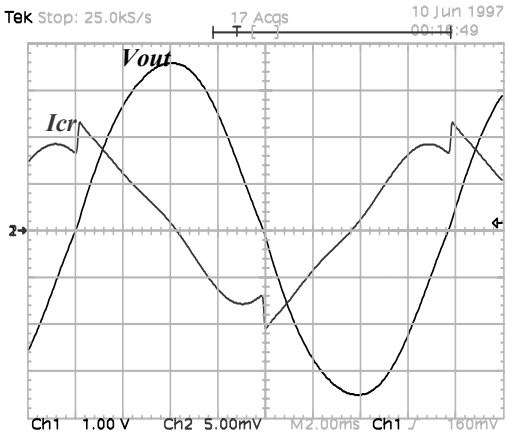

Figure 22. Voltage and current in the resonant capacitor (Steady-state condition)
Scale: 100V/div; 5A/div; 2ms/div

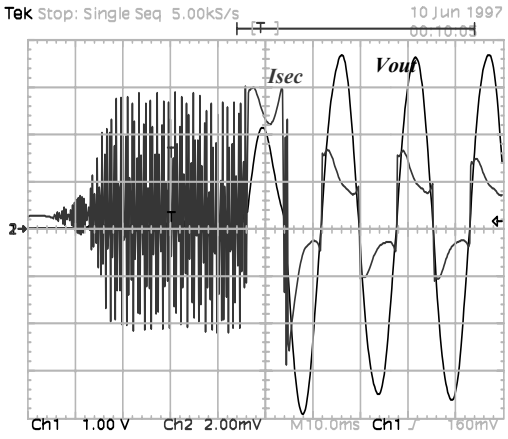

Figure 23. Voltage and current in the secondary Side of the transformer (Start-transient). Scale: 100V/div; 2A/div; 10ms/div

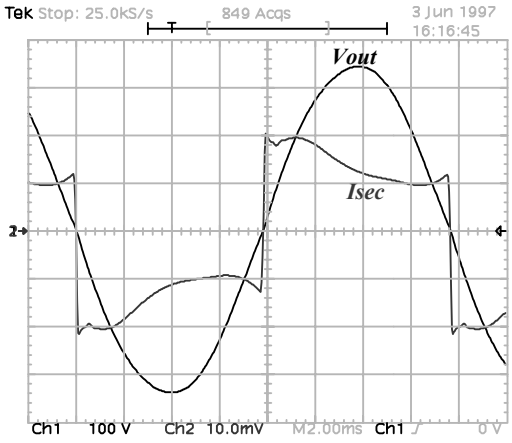

Figure 24. Voltage and current in the Secondary side of the transformer (Steady-state). 100V/div; 1A/div; 2ms/div.

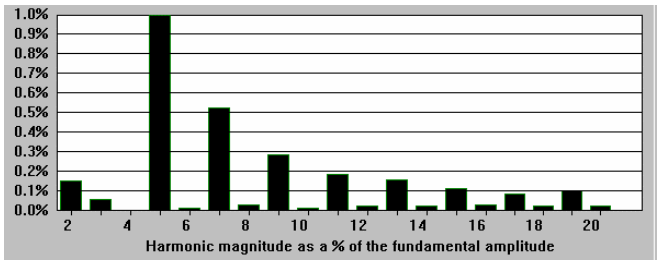

Figure 25. Output voltage harmonic analysis.

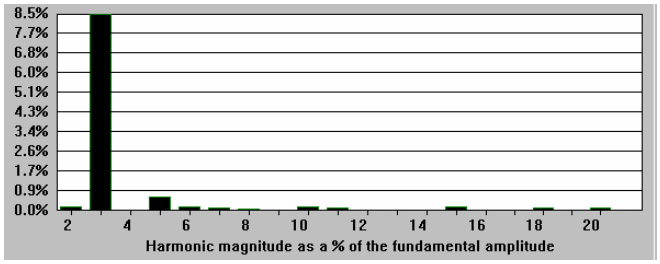

Figure 26. Harmonic analysis of the pump current.

Figures 15 and 16 show the voltage and current in the batteries in the start-transient conditions and steady-state conditions, respectively. The experimental results of the converter show that the voltage across the pump is practically sinusoidal (Fig. 18), with low harmonic distortion (Fig. 25 and 26), and the self-oscillator drive circuit presented good behavior for this application. Besides, the over-voltage across the pump and the Mosfets does not put at risk the structure (Figs. 17, 19 and 20). The start current of the converter is inside the limit specified by the manufacturer of the switches. Figs. 21 and 22 present the voltage and current in the resonant capacitor. The behavior of the voltage and current in the secondary side of the transformer is presented in Figure 23 and in Figure 24.

An efficiency of 91% was obtained at full load condition.

Conclusions

In this paper the analysis of a water pumping system from photovoltaic cells using a current-fed self-oscillator parallel resonant push-pull inverter operating a vibratory under-water pump, for residential applications in rural areas was presented. The converter is shown to be extremely well adapted to this kind of pump, providing sinusoidal voltage with low harmonic distortion without the necessity of any type of modulation. According to the results obtained we have a DC-AC converter with the following features: it is particularly simple and robust, it uses low cost technology, it can operate with only one power processing stage, it has a simple control circuit with its terminals earthed in the same grounding, low harmonic distortion of the load voltage, natural isolation and low number of control switches.

Therefore, the authors believe that this technology can be very useful for some rural residential applications.

References

[1] Muljadi, E. (1997) PV Water Pumping with a Peak-Power Tracker Using a Simple Six-Step Square-Wave Inverter, *IEEE Trans. on Industry Applications,* **33** (3)**,** May/June, 714-721.

[2] Slabbert, C. and Malengret, M. (1998) Grid Connected/ Solar Water Pump for Rural Areas, *Proc. IEEE-ISIE'98*, **1,** 31-34.

[3] Van der Merwe, L. and Van der Merwe, G. J. (1998) Universal Converter for DC PV Water Pumping System, *IEEE-IECON'98*, **1,** 218-223.

[4] Moechtar, M., Juwono, M. & Kantosa, E. (1991) Performance Evaluation of AC and DC Direct Coupled Photovoltaic Water Pumping Systems, *Energy Conservation and Management Journal*, **31** (6), 521-527.

[5] Lee, C. H., Joung,G. B, Cho, G. H. (1990) A Unity Power Factor High Frequency Parallel Resonant Electronic Ballast, *IEEE-IAS*, **2**, 1149-1156.

[6] Brüning, G. (1986) A Comparative Introduction of a New High Voltage Resonant Oscillator, *IEEE-APEC'86*, **1**, 76-82.

[7] Brüning, G. (1986) A New High-Voltage Oscillator, *IEEE Trans. on Industrial Electronics*, **IE-33** (2)**,** May, 171-175.

[8] Mezaroba, M. (1998) Water Pumping System Using the Solar Energy From Photovoltaic Panels Array, *Master Thesis*, INEP/EEL/UFSC, Florianópolis, SC, Brazil.

[9] Pspice Circuit Analysis (1989), Microsim Corporation, version 4.05.